

Interacting classical dimers on the square lattice

Fabien Alet¹, Jesper Lykke Jacobsen^{1,2}, Gregoire Misguich¹, Vincent Pasquier¹, Frederic Mila³, and Matthias Troyer⁴

¹Service de Physique Theorique, CEA Saclay, 91191 Gif sur Yvette, France

²LPTMS, Université Paris-Sud, Bâtiment 100, 91405 Orsay, France

³Institute of Theoretical Physics, Ecole Polytechnique Fédérale de Lausanne, CH-1015 Lausanne, Switzerland and

⁴Theoretische Physik, ETH Zurich, CH-8093 Zurich, Switzerland

(Dated: February 8, 2020)

We introduce a model of close-packed dimers on the square lattice with a nearest neighbor interaction between parallel dimers. This model can be seen as the classical limit of Quantum Dimer Models [D. S. Rokhsar and S. A. Kivelson, Phys. Rev. Lett. 61, 2376 (1988)]. By means of Monte Carlo and Transfer Matrix calculations, we show that this system undergoes a Kosterlitz-Thouless transition separating a low temperature ordered phase where dimers are aligned in columns from a high temperature critical phase with continuously varying exponents. This is understood by constructing the corresponding Coulomb gas, whose coupling constant is computed numerically.

PACS numbers: 05.10.Ln, 05.50.+q, 64.60.Cn, 64.60.Fr

The model of lattice coverings by hard-core dimers has a long history [1] in classical statistical physics, culminating in its solution for arbitrary planar graphs [2], the calculation of correlation functions [3], and its connection to Ising [4] or height models [5, 6]. With the introduction of Quantum Dimer Models (QDM) [7] by Rokhsar and Kivelson [8], and later with the development of this field in connection with Resonating Valence Bond and fractionalization physics in 2D [9] and 3D [10], dimer models have regained interest.

Surprisingly, the effect of interactions between dimers (besides their hard-core repulsion) has not been much studied in the classical case. In this Letter, we investigate the effect on the critical correlations [3], of an interaction that tends to align neighboring dimers. We find that a critical phase with continuously varying exponents exists down to a finite temperature where the dimers order through a Kosterlitz-Thouless (KT) transition [11]. Our results are naturally understood in the Coulomb gas approach [12] to the associated height model [5, 6]. Indeed, this interacting dimer model provides one of the simplest realizations (together with the six-vertex and the XY model) of a Coulomb gas (CG) with continuously varying exponents.

Model and numerical methods | We study a model of interacting dimers on the square lattice, defined by the partition function :

$$Z = \sum_{\text{cog}} \exp \left[-\frac{h}{T} (N^{\circ} \blacksquare) + N^{\circ} (\blacksquare) \right] ; \quad (1)$$

where T is the temperature, the sum runs over all dimer coverings cog of the square lattice, and $N^{\circ} \blacksquare + N^{\circ} (\blacksquare)$ is the number of plaquettes with parallel dimers (either horizontal or vertical) in the configuration c. We consider the case $v = 1$, i.e. aligning interactions between the dimers. Eq. (1) describes the most natural interactions between dimers and corresponds to the diagonal part of the Hamiltonian of the QDM [8]. Our model can there-

fore be interpreted as the classical limit of the QDM.

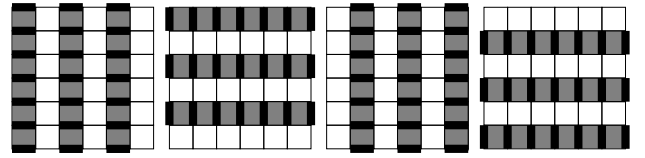


FIG. 1: The four possible columnar ground states. To each plaquette with a pair of parallel dimers we assign an energy of $+v$ (shaded plaquettes in the figure).

At $T = 1$, Eq. (1) describes the classical dimer covering problem, and thus displays critical correlations [3]. At $T = 0$, the dimers order in columns and the ground-state is four-fold degenerate (see Fig. 1): this columnar phase breaks translational and rotational symmetry.

We study Eq. (1) with Transfer Matrix (TM) techniques and with a Monte Carlo (MC) directed loop algorithm [13]. The MC simulations are made on $N = L \times L$ lattices with periodic boundary conditions (PBC).

Transition to the columnar phase | Previous simulations of the QDM on the square lattice found the existence of a plaquette phase (which breaks translational but not π -rotational symmetry) [14]. In the MC simulations of the classical model Eq. (1), we also find important plaquette correlations on finite samples, which nevertheless vanish in the thermodynamic limit [15]. However, they affect the finite-size scaling analysis of the order parameter used in Ref. 16. For this reason we resort to quantities insensitive to plaquette correlations to detect the entrance into the columnar phase. Following Ref. 14, we define the dimer rotational symmetry breaking (DSB) and pair rotational symmetry breaking (PSB) order parameter as :

$$\begin{aligned} \text{DSB} &= N^{-1} \langle N^{\circ} \blacksquare - N^{\circ} (\blacksquare) \rangle \\ \text{PSB} &= N^{-1} \langle N^{\circ} \blacksquare + N^{\circ} (\blacksquare) \rangle; \end{aligned} \quad (2)$$

where $N^{\circ} \blacksquare$ (resp. $N^{\circ} (\blacksquare)$) is the number of horizontal (resp. vertical) dimers in the configuration c. These

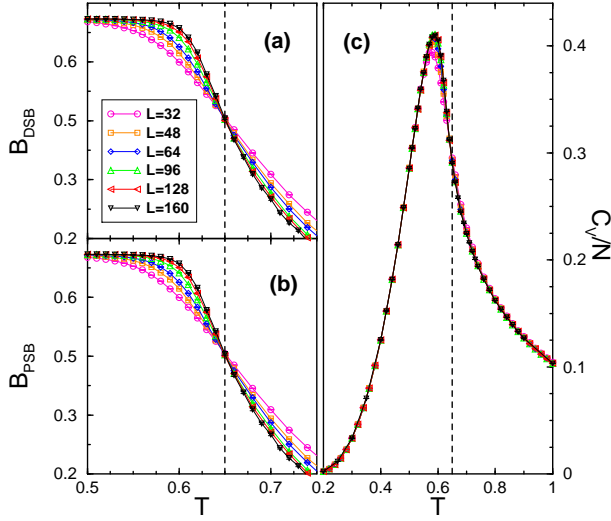


FIG. 2: (Color online) Dimer symmetry breaking cumulant (a), Pair symmetry breaking cumulant (b), and Specific heat per site (c) versus temperature for different system sizes. The dashed lines indicate the estimate $T_c = 0.65(1)$.

two quantities show long-range order in a columnar phase, but vanish in a plaquette phase. To locate with high precision the transition, we study their Binder cumulants [17], defined respectively as $B_{DSB} = 1/\langle h_{DSB}^4 \rangle = (3\langle h_{DSB}^2 \rangle^2)$ and $B_{PSB} = 1/\langle h_{PSB}^4 \rangle = (3\langle h_{PSB}^2 \rangle^2)$; here $\langle \cdot \rangle$ denotes the ensemble average. In the thermodynamic limit, these cumulants saturate to $2/3$ in a long-range ordered phase, and vanish in a disordered phase. They are displayed as a function of temperature T for different system sizes in Figs. 2(a) and 2(b). For both Binder cumulants, the curves for different L all cross at a unique T , which we identify as the transition temperature $T_c = 0.65(1)$ to the columnar phase.

The specific heat per site C_v/N displays a peak, which does not diverge in the thermodynamic limit (see Fig. 2(c)). This points towards a second order transition with a critical exponent $\alpha = 0$, or a KT transition. We also find that the peak of C_v/N is not located at the value of T_c determined by the cumulants (denoted by a dashed line in Fig. 2) but slightly below. A featureless specific heat at the transition point is a strong indication of a KT phase transition.

High temperature phase | We now investigate the nature of the high-temperature phase $T > T_c$. To this end, we calculate the dimer-dimer correlation function

$$G(x) = \langle n_{\square}(r) n_{\square}(r+x) \rangle, \quad l=16; \quad (3)$$

where $n_{\square}(r) = 1$ for an horizontal dimer at site r , and 0 otherwise. The constant $l=16$ stands for the dimer density squared. We take $x = (x; 0)$ and we find in this case that $G(x)$ is staggered with x at any temperature $T > T_c$. We also calculate the monomer-monomer correlation function $M(x)$, proportional to the number

of configurations with two test monomers separated by x [3, 13, 18]. $M(x)$ can be computed in the loop building process of the MC simulation [13]. For a bipartite system, $M(x) = 0$ for monomers on the same sublattice. We again take $x = (x; 0)$, and the normalization such that $M(1) = 1$ [13, 18].

Anticipating on the results, we look for algebraic decay of these correlators for $T > T_c$ and define exponents α_d and α_m by $G(x) \sim |x|^{-\alpha_d}$ and $M(x) \sim |x|^{-\alpha_m}$ for large x . At $T = 1$, we have the exact results [3] $\alpha_d = 2$ and $\alpha_m = 1/2$.

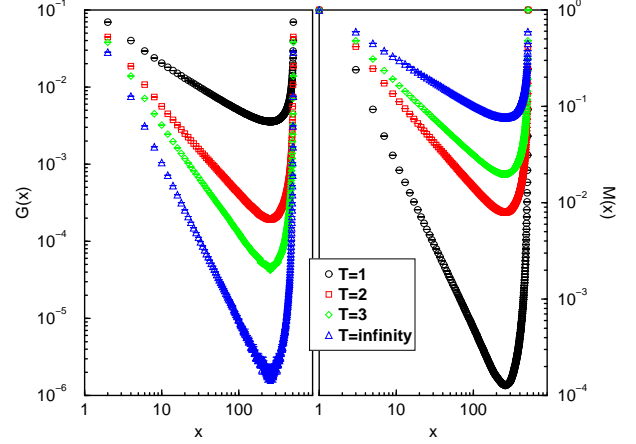


FIG. 3: (Color online) Dimer-Dimer $G(x)$ (left) and Monomer-Monomer $M(x)$ (right) correlation functions versus distance x in a log-log scale for various temperatures.

In Fig. 3, we show $G(x)$ and $M(x)$ calculated on a $L = 512$ sample for various temperatures $T > T_c$. Both correlators indeed show power-law decay for all $T > T_c$, and the exponents α_d and α_m appear to vary continuously with T . The power-law decay is eventually cut around $L=2$ due to the PBC used in the simulations. The T -dependence of the exponents can be estimated from these plots; however the symmetric form of $M(x)$ and $G(x)$ around $L=2$ makes a high precision difficult.

We therefore turn to TM calculations, which are performed on semi-infinite cylinders of even circumference L . By convention, the space coordinate x is horizontal and time t runs upwards. The PBC give $x = x + L$. Place arrows on all lattice edges, such that even (odd) sites are sources (sinks) of four arrows. Define a (staggered) reference configuration c_0 by placing dimers on up-pointing arrows only. Superposing a given configuration c with c_0 gives a transition graph with a conserved number W_x of (oriented) time-like strings. More precisely, $W_x = \sum_x n_{\square}^{\#}(x;t) - n_{\square}^{\#}(x;t) / 2$ if $\frac{1}{2} \leq x \leq \frac{L}{2}$ is independent of t and labels the blocks of the TM. The block $W_x \neq 0$ corresponds to a defect of W_x monomers on the same sublattice at $t = 1$, and W_x monomers on the opposite sublattice at $t = 1$. This can be seen by taking a $W_x = 0$ configuration and shifting its dimers

along some time-like string: this changes W_x by ± 1 and introduces a monomer at either end of the string.

Order the TM eigenvalues as $\lambda_1^{W_x}, \lambda_2^{W_x}, \dots$. We expect λ_1^0 (no monomers) to dominate all other eigenvalues. Using standard predictions of conformal field theory [19], the L -dependence of λ_1^0 gives the central charge c ; the ratio $\lambda_1^0 = \lambda_2^0$ determines d and $\lambda_1^0 = \lambda_1^1$ gives m . Note that the eigenvectors corresponding to λ_1^0 (resp. λ_2^0) are even (resp. odd) under the shift $x \rightarrow x + 1$.

To account for the interactions in Eq. (1), the TM states must encode vertical and horizontal dimer occupancies within a row [15]. We use sparse-matrix factorization, and the state space is built from a reference state in the given W_x -sector by means of hashing techniques. Computations were performed up to $L = 18$, with 1 728 292 states in the $W_x = 0$ sector.

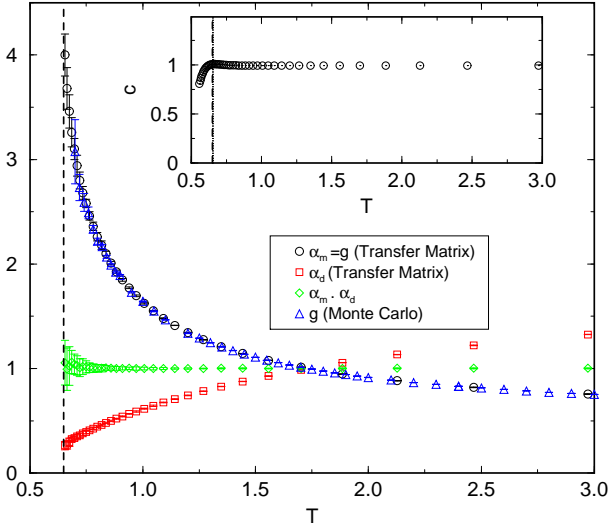


FIG. 4: (Color online) Dimer-dimer α_d and monomer-monomer α_m exponents (and their product) obtained by TM calculations, and coupling constant g of the CG as obtained by MC, all versus temperature T . Inset: Central charge c versus T . The dashed lines denote the MC estimate of T_c .

In Fig. 4, we show α_m and α_d as functions of temperature (error bars are determined from the finite size scaling analysis). α_m increases from $1/2$ at $T = 1$ to $4/3$ at the transition temperature T_c , and then diverges below T_c (not shown in Fig. 4). α_d decreases from 2 at $T = 1$ to 0.26 at T_c , and vanishes below (not shown). We also plot in Fig. 4 the product $\alpha_m \alpha_d$, which equals 1 within error bars for any $T > T_c$. The continuous variation of both α_m and α_d as functions of T indicates criticality for $T_c < T < 1$. This is corroborated by the central charge c as a function of T (see inset of Fig. 4), which is 1.00 in the critical phase and drops abruptly below T_c . T_c can be estimated from the TM by $\alpha_m(T_c) = 4$, the jump in c , or $\alpha_d(T_c) = 1/4$. The exact values quoted are accounted for by the CG formalism dressed below. The first determination is the most precise and gives $T_c = 0.65$ (1), in

full agreement with the MC results.

Coulomb gas representation | The findings above (Kosterlitz-Thouless transition, critical phase with continuously varying exponents) and the dimensionality $d = 2$ of the problem naturally suggest Coulomb gas physics [12]. Here we explain how such a description appears. Close-packed dimers on the square lattice admit a height representation [5, 6], where a height z is assigned (up to an overall constant) to each plaquette in the following way: going counterclockwise around a site on the even sublattice, z changes by $\pm 3/4$ when crossing a dimer and by $\mp 1/4$ across an empty bond. In these units, a monomer corresponds to a dislocation of 1 in the height. To describe the long-wavelength physics of our model, we follow Ref. 6 and coarse-grain the local height variable z to a continuum field $h(r)$, for which we postulate the following action:

$$S = \int dr \left[\frac{g}{2} (\nabla h(r))^2 + V \cos 2\pi h(r) \right] \quad (4)$$

The first term accounts for the cost of fluctuations of the height interface and is dominant in the high- T rough phase. It measures the dimer entropy associated to a given coarse-grained height $h(r)$. The second term is a locking potential that forces the dimers to order in one of the $p = 4$ flat ground states depicted in Fig. 1, which have constant coarse-grained height satisfying $h(r) = 1/8, 3/8, 5/8$ and $7/8$ (mod 1) (these four states correspond to the "ideal states" of Ref. 6). The words "flat" and "rough" match the terminology of height models [5], and the transition between the high- T critical phase and the low- T columnar phase is a roughening transition. The factor $p = 4$ in the periodicity of the locking potential is imposed by the number of ground states in our model (linked here to the elementary height jump $\Delta z = 1/4$ which in turn corresponds to the coordination number of the lattice), g is the CG coupling constant (see the following discussion) [20] and $V > 0$ the strength of the locking potential (the actual value of V is immaterial).

At high T , the locking potential is irrelevant and the long-distance behavior is determined by a free height field. As is well known, this can also be described in terms of a Coulomb gas with electric charges e only. Dual, magnetic charges m correspond to height dislocations, which can be inserted "by hand" through monomers or appropriate boundary conditions (cf. the above discussion of the TM). Units are such that e and m are integers. The exponent of an electromagnetic operator of charge $(e; m)$ reads $\langle e; m \rangle = g^{-1} e^2 + g m^2$ [12]. We identify the leading dimer-dimer and monomer-monomer correlations by $\alpha_d = (1; 0)$ and $\alpha_m = (0; 1)$. The exact results of Ref. 3 then fix the coupling constant $g = 1/2$ at $T = 1$ [6]; in general $g = g(T)$ must depend on T to account for the continuously varying exponents.

More generally, electric charges define the vertex operators $V_e(r) = \exp 2\pi i e h(r)$ appearing in the Fourier

expansion of any operator which is periodic in the coarse-grained height. Note that such a term with $e = 1$ appears as a continuum limit contribution to the dimer operator [21]. The locking potential corresponds to V_p with $p = 4$. When this becomes relevant, the discretization of the height will survive in the continuum limit, and the coarse-grained height can no longer be rough. We can therefore determine $g(T_c) = 4$ from the marginality of V_p , i.e., $(4;0) = 4$.

To check these CG predictions, we calculate g as a function of T . Since $m = g$, we can extract $g(T)$ with high precision from the TM results (see Fig. 4), but it is also accessible via MC calculations of the fluctuations of the winding number $hW^2_i = \frac{1}{2}hW_x^2 + W_y^2$. The winding number W_x (resp. W_y) is the local height difference accumulated by a path winding around the torus with PBC in the x (resp. y) direction. hW^2_i is simply related to g in the free-field point of view [22]. By separating the average tilt from the spatial fluctuations of the height, the partition function is written as a sum over W_x and W_y . The associated Boltzmann weight is given by the action of Eq. (4) evaluated with its classical solution ($\nabla h(r) = 0$) given by a linear height $h(x; y) = \frac{x}{L_x}W_x + \frac{y}{L_y}W_y$ (and $V = 0$). The winding number fluctuations are then

$$hW^2_i = \sum_{n \in 2\mathbb{Z}} \sum_{n' \in 2\mathbb{Z}} n^2 e^{g n^2} = \sum_{n \in 2\mathbb{Z}} e^{g n^2} : \quad (5)$$

In Fig. 4, we show the MC results for g obtained from hW^2_i and Eq. (5), which match with high precision the TM evaluation. This validates the CG scenario for the transition in our model.

In conclusion, we have introduced a model of dimers on the square lattice with an interaction that favors dimer alignment. We find that this model undergoes a KT transition separating a high temperature critical phase with continuously varying exponents from a low temperature crystalline phase. The transition is understood as the roughening transition in the height representation or equivalently as a proliferation of $e = 4$ electric charges in the CG framework. This model is useful in this context since it captures naturally all the contents of the CG: electric (dimers) and magnetic (monomers) charges, and a (temperature-dependent) coupling constant g driving the transition. Natural extensions of our model consist in penalizing dimer alignment (where we expect a transition to a tilted phase), allowing monomers, or considering other geometries. Concerning quantum systems, the rough phase should survive in a large part of the finite-temperature phase diagram of the QDM (above the melting temperatures of the ordered phases) and especially so in the vicinity of the so-called Rokhsar-Kivelson point [8]. We thus expect continuously varying exponents parametrized by a CG coupling constant at sufficiently high temperature, but the detailed finite-temperature

properties of the QDM remain to be explored.

Acknowledgments — We thank W. Knauth, R. Moessner and A. Ralko for fruitful discussions. The MC calculations were performed on the Gallega cluster at SPHt using the ALPS libraries [23].

Electronic address: alet@sph.saclay.cea.fr

- [1] J. K. Roberts, Proc. Roy. Soc. (London) A 152, 464 (1935); R. H. Fowler and G. S. Rushbrooke, Trans. Faraday Soc. 33, 1272 (1937).
- [2] P. W. Kasteleyn, Physica 27, 1209 (1961); H. N. V. Temperley and M. E. Fisher, Phil. Mag. 6, 1061 (1961); M. E. Fisher, Phys. Rev. 124, 1664 (1961).
- [3] M. E. Fisher and J. Stephenson, Phys. Rev. 132, 1411 (1963).
- [4] M. E. Fisher, J. Math. Phys. 7, 1776 (1966).
- [5] H. W. J. Blöte and H. J. Hilhorst, J. Phys. A 15, L631 (1982); B. Nienhuis, H. J. Hilhorst and H. W. J. Blöte, *ibid.* 17, 3559, (1984).
- [6] J. Kondev and C. L. Henley, Nucl. Phys. B 464, 540 (1996); R. Raghavan, C. L. Henley and S. L. Aroh, J. Stat. Phys. 86, 517 (1997).
- [7] In a QDM, dimer coverings form a basis of the Hilbert space. Dimers gain some kinetic energy by hopping around plaquettes (resonance) and experience some interaction (repulsive or attractive).
- [8] D. S. Rokhsar and S. A. Kivelson, Phys. Rev. Lett. 61, 2376 (1988).
- [9] R. Moessner and S. L. Sondhi, Phys. Rev. Lett. 86, 1881 (2001); G. Misguich, D. Serban and V. Pasquier, *ibid.* 89, 137202 (2002); R. Moessner, S. L. Sondhi and E. Fradkin, Phys. Rev. B 65, 024504 (2002); D. A. Ivanov, *ibid.* 70, 094430 (2004).
- [10] R. Moessner and S. L. Sondhi, Phys. Rev. B 68, 184512 (2003).
- [11] J. M. Kosterlitz and D. J. Thouless, J. Phys. C 6, 1181 (1973); V. L. Berezinskii, Sov. Phys. JETP 32, 493 (1971).
- [12] B. Nienhuis, in Phase transitions and Critical Phenomena, edited by C. Domb and J. L. Lebowitz (Academic, London, 1987), Vol. 11.
- [13] A. Sandvik, E-print cond-mat/0312097.
- [14] P. W. Leung, K. C. Chiu and K. J. Runge, Phys. Rev. B 54, 12938 (1996).
- [15] F. Alet et al., in preparation.
- [16] S. Sachdev, Phys. Rev. B 40, 5204 (1989).
- [17] K. Binder, Z. Phys. B 43, 119 (1981).
- [18] W. Knauth and R. Moessner, Phys. Rev. B 67, 064503 (2003).
- [19] J. L. Cardy, J. Phys. A 17, L385 (1984); H. W. J. Blöte, J. L. Cardy, and M. P. Nightingale, Phys. Rev. Lett. 56, 742 (1986); I. A. Ieck, *ibid.* 56, 746 (1986).
- [20] We use here the notations of Ref. 12. g is related to the stiffness constant K used in Ref. 6 by $g = 8K = \dots$
- [21] E. Fradkin et al., Phys. Rev. B 69, 224415 (2004).
- [22] S. K. Yang, Nucl. Phys. B 285, 183 (1987); P. Di Francesco, H. Saleur and J.-B. Zuber, J. Stat. Phys. 49, 57 (1987).
- [23] F. Alet et al., E-print cond-mat/0410407; M. Troyer, B. Ammon and E. Heeb, Lect. Notes Comput. Sci., 1505, 191 (1998). Source codes can be obtained from <http://alps.compphys.org>